

1 **Cytoneuclear Discordance and Historical Demography of Two Brown Frogs, *Rana tagoi***
2 **and *R. sakuraii* (Amphibia: Ranidae)**

3

4 KOSHIRO ETO and MASAFUMI MATSUI*

5

6 *Graduate School of Human and Environmental Studies, Kyoto University, Yoshida*

7 *Nihonmatsu-cho, Sakyo-ku, Kyoto 606-8501, Japan*

8

9 *Corresponding author. Phone: +81-75-753-6846;

10 FAX: +81-75-753-6846;

11 E-mail: fumi@zoo.zool.kyoto-u.ac.jp

12

13 **Abstract**

14 Prior studies of mitochondrial genomic variation reveal that the Japanese brown frog *Rana*
15 *tagoi* comprises a complex of cryptic species lineages, and that *R. sakuraii* arose from within
16 this complex. Neither species forms a monophyletic group on the mitochondrial haplotype tree,
17 precluding a simple explanation for the evolutionary origins of *R. sakuraii*. We present a more
18 complete sampling of mitochondrial haplotypic variation (from the *ND1* and *16S* genes) plus
19 DNA sequence variation for five nuclear loci (from the genes encoding *NCX1*, *NFIA*, *POMC*,
20 *SLC8A3*, and *TYR*) to resolve the evolutionary histories of these species. We test hypotheses of
21 population assignment (STRUCTURE) and isolation-with-migration (IM) using the more
22 slowly evolving nuclear markers. These demographic analyses of nuclear genetic variation
23 confirm species-level distinctness and integrity of *R. sakuraii* despite its apparent polyphyly on
24 the mitochondrial haplotype tree. Divergence-time estimates from both the mitochondrial
25 haplotypes and nuclear genomic markers suggest that *R. sakuraii* originated approximately one
26 million years ago, and that incomplete sorting of mitochondrial haplotype lineages best explains

27 non-monophyly of *R. sakuraii* mitochondrial haplotypes. Cytonuclear discordance elsewhere in
28 *R. tagoi* reveals a case of mitochondrial introgression between two species lineages on Honshu.
29 The earliest phylogenetic divergence within this species group occurred approximately four
30 million years ago, followed by cladogenetic events in the Pliocene and early Pleistocene
31 yielding 10–13 extant species lineages, including *R. sakuraii* as one of the youngest.

32

33 Key words: species complex; incomplete lineage sorting; introgression; isolation with migration

34

35 **1. Introduction**

36 Japanese brown frogs *Rana tagoi* and *R. sakuraii* are known to show a complicated
37 genealogical relationship (Tanaka et al., 1996; Eto et al., 2012, 2013). *Rana tagoi* occurs widely
38 on the main and peripheral islands of the Japanese archipelago except for Hokkaido and the
39 Ryukyus. While most brown frogs breed in open, still waters, *R. tagoi* breeds in subterranean
40 streams where the larvae can metamorphose without feeding (Matsui and Matsui, 1990; Maeda
41 and Matsui, 1999). These distinctive traits might be the product of adaptation to the
42 mountainous environments of the Japanese archipelago. Conversely, *R. sakuraii*, occurring only
43 on Honshu sympatric with *R. tagoi*, breeds under rocks in open streams, and adult frogs have
44 several characters suitable for a lotic environment (e.g., they possess fully developed toe webs,
45 which are less well developed in *R. tagoi*), although its eggs and larvae share traits with those of
46 *R. tagoi*. From these facts, Matsui and Matsui (1990) postulated that *R. sakuraii* speciated from
47 a *R. tagoi*-like ancestor when it adapted to stream environments. This hypothesis is supported
48 by phylogenetic analyses of mitochondrial haplotypes, in which *R. sakuraii* is embedded in *R.*
49 *tagoi* lineages (Tanaka et al., 1996; Eto et al., 2012). However, neither of the species is
50 monophyletic on the mitochondrial haplotype tree (Eto et al., 2012). Mitochondrial haplotype
51 variation reveals that *R. tagoi* is divided into numerous species lineages, and some of these
52 lineages are reproductively isolated from each other (Eto et al., 2012, 2013). As is clear from

53 these studies, *R. tagoi* contains multiple cryptic species, one of which is the sister taxon to *R.*
54 *sakurarii*. Two hypotheses potentially explain polyphyly of *R. sakurarii* haplotypes on the
55 mitochondrial haplotype phylogeny. Incomplete lineage sorting (ILS), retention of disparate
56 haplotype lineages from an *R. tagoi*-like ancestor, is the simplest explanation if *R. sakurarii*
57 originated very recently, within the past approximately one million years. Alternatively,
58 introgression of mitochondrial haplotypes resulting from gene flow between *R. sakurarii* and a
59 sympatric lineage of *R. tagoi* could explain the anomalous phylogenetic distribution of *R.*
60 *sakurarii* mitochondrial haplotypes.

61 In this study, we analyse sequence data for two mitochondrial and five nuclear loci to test
62 these hypothesis and to estimate divergence times and demographic patterns of these two
63 species. Expanded sampling of mitochondrial haplotype variation relative to earlier studies
64 yields increased precision of the mitochondrial phylogenetic analysis. We test hypotheses of
65 population assignment (Pritchard et al, 2000) and isolation-with-migration (IM; Hey, 2010)
66 using the more slowly evolving nuclear markers to verify inferences made from the
67 mitochondrial haplotype phylogeny.

68

69 **2. Materials and Methods**

70 *2.1. Sampling strategy*

71 For each species, we chose samples belonging to representative localities/mt-lineages based
72 on previous studies (e.g., Eto et al., 2012). We analysed 107 samples of *R. tagoi* (including three
73 samples each of the subspecies *R. t. yakushimensis* and *R. t. okiensis* from peripheral islands)
74 and 21 of *R. sakurarii* from 81 localities (Fig. 1, Table S1). To the mtDNA phylogenetic analysis,
75 we added GenBank data for *R. kobai* (AB685768), *R. sauteri* (AB685767), *R. tsushimensis*
76 (AB639592, AB639752), and *R. ulma* (AB685780) as outgroup taxa based on known
77 phylogenetic relationships (Tanaka-Ueno et al., 1996, 1998).

78

79 2.2. Sequencing of DNA

80 Total DNA was extracted from frozen or ethanol-preserved tissues using standard phenol-
81 chloroform extraction procedures. Then, we amplified fragments containing the target region
82 (two mitochondrial genes, 16S ribosomal RNA [*16S*] and NADH dehydrogenase subunit 1
83 [*ND1*]; and five nuclear genes, sodium-calcium exchanger 1 [*NCX1=SLC8A1*], nuclear factor
84 I/A [*NFIA*], pro-opiomelanocortin [*POMC*], sodium-calcium exchanger 3 [*SLC8A3*], and
85 tyrosinase [*TYR*]) by polymerase chain reaction (PCR). The experimental conditions and PCR
86 techniques were essentially identical to those reported previously (Eto et al., 2012). The
87 amplified PCR products were purified by polyethylene glycol (PEG) precipitation. The cycle
88 sequence reactions were performed out with an ABI PRISM Big Dye Terminator ver. 3.1 Cycle
89 sequencing Kit (Applied Biosystems) and sequenced on an ABI 3130 automated sequencer. We
90 used the primers listed in Table S2 for PCR and sequencing, and all samples/loci were
91 sequenced in both directions.

92

93 2.3. Alignment of DNA, haplotype determination, and data characteristics

94 Sequence alignment was conducted using MUSCLE (Edgar, 2004). For heterozygous
95 nuclear genes, we used PHASE ver. 2.1 (Stephens et al., 2001) to determine haplotypes. In this
96 analysis, the threshold of probability was set to small values (0.5–0.6) following Garrick et al.
97 (2010). Before analysing the historical demography, we also used IMgc (Woerner et al., 2007)
98 to detect the largest non-recombining block of nDNA for IM analysis, because IMA2 assumes
99 no intra-locus recombination (Hey and Nielsen, 2004). As data parameters, we calculated the
100 summary statistics of variable sites (vs), number of haplotypes (h), haplotype diversity (H_d), and
101 nucleotide diversity (π). We also checked the neutrality of the five nuclear loci with Tajima's D
102 (Tajima, 1989). Since none of them showed significant deviation from zero (Table S3), these
103 loci were considered neutral markers. We conducted all of these calculations using DnaSP
104 (Rozas et al., 2003).

105

106 *2.4. Population assignment based on mtDNA*

107 A phylogenetic analysis was conducted using the two mitochondrial genes. First, we
108 selected the best substitution model for each gene using Kakusan4 (Tanabe, 2011) based on the
109 Akaike information criterion (AIC). Then, phylogenetic trees based on the maximum-likelihood
110 method (ML) and Bayesian inference (BI) were constructed using TREEFINDER ver. Mar.
111 2011 (Jobb, 2011) and MrBayes ver. 3.2.1 (Ronquist and Huelsenbeck, 2003), respectively. For
112 the ML tree, we conducted non-parametric bootstrap analysis with 1000 replicates, and
113 branches with a bootstrap value (BS) of 70% or greater were regarded as significantly supported.
114 In the BI analysis, two independent runs of four Markov chains were conducted for 10 million
115 generations (sampling frequency one tree per 100 generations); the first three million
116 generations were discarded as burn-in. Convergence of parameters was checked using Tracer
117 ver. 1.5 (Rambaut and Drummond, 2009). We considered a Bayesian posterior probability
118 (BPP) of 0.95 or greater as significant support. From the results of both analyses, we used
119 mitochondrial haplotype clades, levels of haplotype divergence, and geographic distributions to
120 diagnose hypothetical species lineages, which were treated as population units based on mtDNA
121 in the later analyses.

122

123 *2.5. Population assignment based on nDNA*

124 *Rana tagoi* and *R. sakurarii* are so close genetically as to cause difficulty constructing
125 phylogenetic trees using nDNA sequences (Eto et al., 2012, 2013). Therefore, we conducted
126 clustering analysis using STRUCTURE ver. 2.3.3 (Pritchard et al., 2000) to delimit population
127 units based on nDNA. We applied an admixture and allele-frequency-independent model to
128 haplotype data for the nuclear loci, and calculated 500,000 generations following 100,000
129 generations of burn-in. The number of clusters (K) was set from 1 to 10, and 10 independent
130 iterations were conducted for each K . The most likely K was determined by the likelihood

131 distribution of each iteration and the delta K value (Evanno et al., 2005). We also constructed
132 haplotype networks for each gene based on the median-joining method using Network ver. 4.6
133 (Bandelt et al., 1999) to examine the relationships among nuclear haplotypes.

134

135 2.6. Divergence dating based on mtDNA

136 To estimate the divergence time between mt-lineages, we conducted Bayesian analysis
137 using BEAST ver. 1.7.5 (Drummond et al., 2012). For each calibration, 10 million generations
138 of run (of which the first three million were discarded as burn-in) were conducted under a non-
139 autocorrelated log-normal relaxed clock model. Tracer ver. 1.5 (Rambaut and Drummond,
140 2009) was used to check the parameter distributions and effective sample size. We applied the
141 following two different calibrations:

142 **Calibration I:** The molecular evolutionary rate of 1.38% (0.69% per lineage) per MY was
143 applied. This value was estimated for the *ND1* and *ND2* regions of *Bufo* (Macey et al., 1998),
144 and only *ND1* data were used in this calculation. The evolutionary rate of this region is similar
145 among a wide range of vertebrates (Macey et al., 2001). We thus used that rate, despite
146 considerable phylogenetic distance between *Rana* and *Bufo*.

147 **Calibration II:** Using only *16S* data, we applied the evolutionary rate of 0.66% (0.33% per
148 lineage) per MY estimated for *16S* of *Leiopelma* (Fouquet et al., 2009).

149

150 2.7. Estimation of historical demography

151 The historical demography, especially the patterns of gene flow and divergence times
152 among species or genetic groups, was examined using coalescent analysis with the Bayesian IM
153 model. We analysed the nDNA data using the program IMA2 (Hey 2010), and estimated the
154 effective population size, N_e , population migration rate, $2N_eM$, and population divergence time,
155 T . As the mutation rate of nuclear genes, we applied 0.047% per MY per lineage for *NCX1*
156 (reported in the genus *Hydromantes*; Rovito 2010), 0.072% (0.061–0.083%) for *POMC*

157 (*Hyperolius*; Lawson, 2010), and 0.047% (0.027–0.067%) for *SLC8A3* (amphibians in general;
158 Roelants et al., 2007). The geometric mean of these values, approximately 2.71×10^{-7} mutations
159 per year per locus, was used as the mutation rate (μ) to scale each demographic parameter.
160 Based on several test runs, the upper bounds for the parameters were set at $\theta = 10\text{--}20$, $t = 3\text{--}5$,
161 and $m = 10\text{--}25$, and five million steps (sampling frequency one tree per 50 steps) of
162 calculations were performed for 30 heated chains after two million burn-in steps. We conducted
163 three independent runs, and finally combined the results using the L-mode option of IMA2.
164 Since *R. tagoi* and *R. sakurarii* typically start to breed at the age of 3 years (Kusano et al., 1995a,
165 b), we applied this value as the generation time of the two species. The trendline plots and
166 effective sample sizes were monitored to ensure good mixing and convergence of parameters.

167 The significance of $2N_eM$ was determined using the log-likelihood ratio (LLR) test of
168 Nielsen and Wakeley (2001). We also used the parameter comparison option (with the -p6
169 command) of IMA2 and output the list of probability, which indicates one parameter to be
170 greater than the other. The relative strength of genetic isolation was evaluated using $2N_eM$
171 values (strong [$2N_eM \leq 1$], moderate [$1 < 2N_eM \leq 5$], and weak [$5 < 2N_eM \leq 25$]: Wright, 1931;
172 Waples and Gaggiotti, 2006; Reilly et al., 2012).

173

174 **3. Results**

175 *3.1. Sequence characteristics*

176 We obtained complete mitochondrial *I6S* (1612bp) and *NDI* (967bp) sequences for all
177 samples. There were 489 parsimoniously informative sites within the ingroup: 244 for *I6S* and
178 245 for *NDI*. The other statistics are listed in Table S3.

179 In the sequences of the five nuclear loci for all 128 samples, only *POMC* had in-dels, and
180 these sites were omitted from the subsequent analyses. For haplotype determination using
181 PHASE, all haplotypes in all samples/loci were determined successfully, except for one sample
182 for *POMC* and two for *TYR*, which were treated as null alleles in subsequent analyses. The

183 sequence length and statistics of each locus are listed in Table S3. Overall, each parameter
184 generally indicated great genetic diversity in *R. tagoi* and *R. sakurarii*. Of the five nuclear loci,
185 *TYR* was the most variable ($H_d = 0.955$ and $\pi = 0.017$ for all samples) and *NFIA* was the least
186 variable (0.735 and 0.003, respectively).

187

188 3.2. Population assignment: Mitochondrial DNA results

189 The best substitution model selected in the ML analysis was the general time reversible
190 (GTR; Tavaré, 1986) model with the optimized gamma shape parameter (G) of 0.158 and the
191 proportion of invariable sites (I) of 0.144 for *I6S* and the J1 (Jobb, 2011) model + G (0.543) + I
192 (0.312) for *NDI*. For BI, the models were GTR + G (0.082) + I (0.226) and GTR + G (0.892) +
193 I (0.226) for *I6S* and *NDI*, respectively. The constructed ML ($-\ln L = 15500.618$) and BI
194 (15863.190) trees were essentially identical in topology, and only the ML tree is shown in Fig. 2.
195 We followed Eto et al. (2012) for the names of each genetic group.

196 The phylogenetic relationships obtained were fundamentally identical to those reported by
197 Eto et al. (2012). The ingroup was divided into two large haplotype clades (A and B), and both
198 of these included subclades judged by their geographic distributions to diagnose separate
199 species lineages (A-1ab to A-9abc and B-1 to B-2ab); Clade B (ML-BS = 82% and
200 BPP = 1.00) contained only haplotypes from *R. tagoi*, while Clade A (ML-BS = 93% and
201 BPP = 1.00) included both *R. tagoi* and *R. sakurarii* haplotypes. Each clade/lineage was well
202 supported (ML-BS $\geq 70\%$, BPP ≥ 0.95). The statistical support for nodes was generally better
203 than in the previous study, and more detailed phylogenetic relationships were clarified,
204 particularly those among the lineages in Clade A. In Clade A, the lineages from Honshu Island
205 (A-1ab to A-6) formed a subclade (A' in Fig. 2. ML-BS = 73% and BPP = 0.98) against the
206 Shikoku and Kyushu subclade (A"; ML-BS = 79% and BPP = 0.95). Within Subclade A', three
207 additional lineage groups were recognised: one consisted of Lineages A-1a and A-1b (ML-
208 BS = 82% and BPP = 1.00); the second of Lineages A-2 and A-3 (ML-BS = 70% and

209 BPP = 0.98); and the third Lineages A-4, A-5, and A-6 (ML-BS = 79% and BPP = 1.00). The
210 haplotypes obtained from *R. sakurarii* were included in Lineages A-2 and A-3. Lineage A-2 also
211 contained *R. tagoi* haplotypes, although haplotypes were not shared between the two species.

212

213 3.3. Population assignment: Nuclear DNA results

214 The results of the clustering analysis using STRUCTURE are shown in Fig. 3. For all
215 samples, $K = 2$ was supported by the test of delta K , and two clusters (I and II) were recognised.
216 Almost all samples were clearly assigned to each cluster (posterior probabilities $\geq 80\%$),
217 indicating strong genetic isolation between the two nDNA clusters. Although the division of the
218 two nuclear clusters (I and II) did not completely correspond to that of the two mitochondrial
219 clades (A and B), Cluster II was largely concordant with mitochondrial Subclade A', with the
220 exception of Lineage A-1a (Fig. 3). Clusters I and II also were separated on the haplotype
221 networks of some nuclear genes (e.g., *NCX1*, *NFIA*, and *SLC8A3*; Fig. S1). However, in
222 relatively more variable genes like *TYR*, the haplotype relationships were highly complex and
223 their separation was not clear (Fig. S1). Furthermore, haplotypes were more or less shared
224 between Clusters I and II in all loci, indicating ILS in these nuclear genes.

225 Since the two large clusters seemed to contain several subclusters, we independently
226 reanalysed samples for the two clusters. Within Cluster I, the population assignment with $K = 2$
227 was supported (Fig. 3). In this clustering, the division of subclusters was still roughly correlated
228 with the mt-lineages: the lineages from the main islands (A-1a, A-7, A-9a, and B-2ab) tended to
229 form a subcluster and the lineages from the peripheral islands (A-8, A-9c, and B-1) formed
230 another. One lineage, A-9b, included samples assigned to both of these subclusters. Except for
231 Lineage A-9b, samples of the two subclusters were clearly assigned to either subcluster. In
232 contrast, $K = 3$ was supported within Cluster II using the delta K test and likelihood distribution.
233 In this division, *R. tagoi* Lineages A-1b and A-4, *R. tagoi* A-2, and *R. sakurarii* (A-3 and part of
234 A-2) each formed a subcluster (Fig. 3). The separation of these subclusters was clear (posterior

235 probabilities > 80%), with a few exceptional samples in the *R. sakurarii* subcluster. By contrast,
236 many samples of lineages A-5 and A-6 were not clearly assigned to particular subclusters, and
237 showed intermediate genetic structures between *R. tagoi* of A-2 and *R. sakurarii*.

238

239 3.4. Divergence times of the mitochondrial lineages

240 The results of divergence dating for the major nodes on the mitochondrial genealogy are
241 listed in Table 1. Although we applied the evolutionary rates of phylogenetically remote taxa
242 (*Bufo* and *Leiopelma*) the divergence times obtained for the ingroup were similar in the two
243 calibrations. Two major mt-clades (A and B: node 1 in Fig. 2) were estimated to have diverged
244 4.2–4.0 (95% highest posterior density interval [HPD] of 6.2–2.3) MYA. Then Subclades A'
245 and A'' (node 2) split 2.8–2.6 (4.1–1.6) MYA, followed by the separation within Clade B (node
246 22) 2.7–2.3 (4.3–1.2) MYA. The two lineages including *R. sakurarii* samples, A-2 and A-3,
247 separated from each other 2.1–1.9 (3.1–1.1) MYA (node 7), followed by internal divergence
248 during 1.4–0.9 (2.2–0.4) MYA (nodes 8 and 9). The most recently divergent lineages were B-2a
249 and B-2b (node 23), which split at 1.4 (2.2–0.7) MYA. These estimates indicate that the
250 divergence of each major mitochondrial clade/lineage began in the mid-to-late Pliocene and was
251 approaching completion in the mid Pleistocene.

252

253 3.5. Historical demography

254 As shown above, the results of the population assignment were not completely concordant
255 between mt- and n-DNA (Figs. 2 and 3). In estimating demographic parameters, we used only
256 nDNA data because nuclear markers are thought to be more conservative than mitochondrial
257 ones, which are more likely to be affected by introgression than the nuclear markers (Ballard
258 and Whitlock 2004).

259

260 3.5.1. *Historical demography between Clusters I and II*

261 First, we conducted a coalescent analysis using IMA2 for the two large nuclear clusters: I
262 and II. Each parameter showed single peaks in their probability density distributions (Fig. S2).
263 The parameter values obtained are listed in Table 2. The estimated population migration rate
264 ($2N_eM$) for I to II ($I \rightarrow II$) was 0.52 (0.24–1.12). In the opposite direction; *i.e.* $II \rightarrow I$, the
265 parameter value tended to be larger, with $2N_eM_{II \rightarrow I}$ being 1.23 (0.70–2.14). The LLR test
266 showed that all of these values were significantly larger than zero ($p < 0.01$), suggesting that
267 clusters I and II have maintained a degree of gene flow after their divergence. However, strong
268 to moderate genetic isolation would exist between the two clusters because the $2N_eM$ values
269 obtained were relatively small (ca. 1 or smaller: Wright, 1931; Waples and Gaggiotti, 2006;
270 Reilly et al., 2012). The effective population size estimated for I, II, and their ancestor was 2.2
271 (1.7–2.9), 1.7 (1.3–2.3), and 0.4 (0.2–0.8) million individuals, respectively. The ancestral
272 population size was smaller than those at present, as supported by parameter comparison of θ
273 (the posterior probabilities were 1.00 for each comparison). The population size of II tended to
274 be smaller than that of I, but the tendency was not supported statistically (BPP < 0.95). The
275 population divergence time (T) of I and II was estimated as 2.7 (4.4–2.2) MYA. Although its
276 95%HPD was relatively wide, this estimate was younger than the divergence time of the two
277 major mt-clades (A/B; ca. 4.2–4.0 MYA), but almost equal to those of A'/A" (ca. 2.8–2.6 MYA)
278 and B-1/B-2 (ca. 2.7–2.3 MYA) (Table 1).

279

280 3.5.2. *Historical demography between R. tagoi and R. sakuraii*

281 Then, we compared demographic parameters between *R. tagoi* and *R. sakuraii*. As *R. tagoi*
282 (R_t), we chose mt-Lineages A-2, 5, and 6, which were genetically close to *R. sakuraii* (R_s) in
283 the mitochondrial and nuclear DNA analyses, as shown above (see Figs. 2 and 3). Since our
284 dataset was not sufficiently informative to analyse a four-populations model, we combined
285 Lineages A-5 and A-6 as a single group; these showed close genetic relationships in both

286 mitochondrial and nuclear analyses (Figs. 2, 3). We conducted two separate analyses under
287 different population schemes: (1) three-populations model, in which *R. sakurarii* (*Rs*) and *R.*
288 *tagoi* (*Rt*) Lineage A-2 were assumed to be mutually close compared to A-5 and 6, based on the
289 mtDNA genealogy, and (2) two-populations model based on the current classification (*Rs* vs. *Rt*
290 A-2, 5, and 6).

291 In the three-populations model, significant gene flow ($p < 0.05$ in the LLR test) was
292 detected only in *R. tagoi* A-5+6 \rightarrow A-2 ($2N_eM_{Rt\ A-5+6 \rightarrow Rt\ A-2}$ was 3.79 [0.75–9.50]; Fig. S3 and
293 Table 2) and A-5+6 \rightarrow *R. sakurarii* ($2N_eM_{Rt\ A-5+6 \rightarrow Rs}$ was 0.40 [0.04–2.00]), and no significant
294 gene flow was recognized between *R. sakurarii* and *R. tagoi* A-2 ($p > 0.05$). These results
295 indicated that the genetic isolation between *R. tagoi* A-2 and A-5+6 was moderate ($1 < 2N_eM \leq$
296 5), but the gene flow was strongly biased to one direction (from A-5+6 to A-2). Although gene
297 flow existed between the two species, the direction was limited (*R. tagoi* A-5+6 \rightarrow *R. sakurarii*),
298 and the population migration rate obtained was small ($2N_eM \leq 1$), indicating strong genetic
299 isolation between *R. sakurarii* and *R. tagoi* lineages. The estimated effective population size (a
300 million individuals) was similar between *R. tagoi* A-2 (0.80 [0.34–2.06]) and A-5+6 (0.79
301 [0.38–1.76]), but was smaller in *R. sakurarii* (0.16 [0.07–0.32]). This tendency was supported in
302 the statistical test, in which N_e for *R. sakurarii* was significantly smaller than those for *R. tagoi*
303 lineages (BPP > 0.95).

304 We could not obtain a sufficient estimate for gene flow between the ancestral populations
305 because no obvious peaks of probability for the parameter $2N_eM$ were recognised (Table 2). The
306 estimated ancestral population size (N_e) was 0.21 (0.01–4.06) for *R. sakurarii* + *R. tagoi* A-2, and
307 was 0.43 (0.23–0.77) for the common ancestor of *R. sakurarii*, *R. tagoi* A-2 and A-5+6. The
308 estimated N_e for the ancestors tended to be smaller than the present N_e for *R. tagoi* (A-2, A-5+6)
309 and larger than that for *R. sakurarii*, but the tendencies were not supported statistically (BPP $<$
310 0.95). The time of population divergence estimated for *R. sakurarii*/*R. tagoi* A-2 (1.1 [2.3–0.6]

311 MYA) was much younger than that for the ancestors (2.15 [6.11–1.31] MYA), although the
312 credibility intervals largely overlapped.

313 In the two-populations model, significant gene flow from *R. tagoi* to *R. sakuraii* was again
314 detected ($2N_eM_{Rt \rightarrow Rs}$ was 0.51 [0.14–1.17]; Fig. S3 and Table 2), but such trend was not
315 recognized in the opposite direction (Fig. S3 and Table 2). These results indicate strong to
316 medium isolation between the two species, although small and unidirectional gene flow exists.
317 The $2N_eM$ value for *R. tagoi* \rightarrow *R. sakuraii* in this model was similar to the value for *R. tagoi* A-
318 5+6 \rightarrow *R. sakuraii* in the three-populations model shown above (Table 2).

319 The estimated N_e showed values and tendencies similar to those obtained in the three-
320 populations model; N_e for *R. sakuraii* (0.17 [0.09–0.34]) was significantly smaller (BPP > 0.95)
321 than that of *R. tagoi* (1.61 [0.99–2.65]). The estimates for ancestral N_e (0.37 [0.10–0.68] in the
322 two-populations model) also are similar between the models. The divergence time estimated for
323 the two species, 1.2 (2.9–0.6) MYA, was slightly older than that estimated by the three-
324 population model (ca. 1.1 MYA).

325

326

327 **4. Discussion**

328 *4.1. Discordance between the classification and patterns of genetic variation using different*
329 *markers*

330 Our new data and analyses confirmed the major patterns of mitochondrial genomic variation
331 reported previously (Eto et al., 2012). Mitochondrial haplotypes obtained from *R. sakuraii* were
332 genealogically embedded in those from *R. tagoi*, and neither species was monophyletic on the
333 haplotype tree. The mitochondrial and nuclear data considered together indicate that *R. sakuraii*
334 constitutes a single species lineage. *Rana sakuraii* corresponds largely to Lineage A-3 on the
335 mitochondrial haplotype tree (Fig. 2), with its sister lineage being *R. tagoi* populations bearing
336 mitochondrial haplotypes of Lineage A-2. Nonetheless, Lineage A-2 includes some *R. sakuraii*

337 mitochondrial haplotypes. We examine the hypotheses of incomplete lineage sorting and gene
338 flow as possible explanations for this pattern. The following three scenarios could explain the
339 phylogenetic pattern of mitochondrial haplotypes of lineages A-2 and A-3 (Fig. 2): (1) recent
340 speciation of *R. sakurarii* from *R. tagoi* Lineage A-2, which led to ILS of mtDNA at the species
341 level; (2a) past mitochondrial introgression from *R. tagoi* A-2 to *R. sakurarii*; and (2b)
342 introgression in the opposite direction (Fig. 4). If recent separation of *R. sakurarii* from *R. tagoi*
343 A-2 was the case, the ILS hypothesis (1) would be the simplest explanation. However, if the
344 speciation was shown to be old, especially much older than the divergence time within mt-
345 Lineage A-2, this hypothesis would be rejected. Conversely, the past-introgression hypotheses
346 (2) would be applicable if the speciation of the two species coincided with the split between
347 Lineages A-2 and A-3 (2a), or the separation of these two lineages from the others (2b).
348 Detection of historical gene flow between *R. sakurarii* and *R. tagoi* A-2 for the nuclear markers
349 also would support the past introgression hypotheses.

350 The genetic relationship based on the STRUCTURE analysis using nDNA was discordant
351 with the mitochondrial genealogy, and *R. sakurarii* and *R. tagoi* A-2 tended to be separated in
352 different subclusters (Fig. 3). This result likely reflects their heterospecific status. The
353 demographic analysis using Ima2 showed that the separation of *R. sakurarii* from *R. tagoi*
354 lineages (ca. 1.1 MYA and 1.2 MYA in three- and two-populations models, respectively; Table
355 2) was younger than the separation of mt-Lineages A-2 and A-3 (ca. 2.1–1.9 MYA; Table 1),
356 and was similar to the divergence within these lineages (ca. 1.4–0.9 MYA). The date of
357 speciation would correspond to, or be younger than, the population divergence time estimated
358 by Ima in this case. So these results favour the ILS hypothesis, although the credibility intervals
359 of these estimates overlapped.

360 Based on the genealogy obtained (Fig. 2), mitochondrial introgression between *R. tagoi* A-2
361 and *R. sakurarii* happened several times if the hypotheses 2 were the case (for example, two
362 independent introgression events should be presumed in the hypothesis 2a). Thus the

363 introgression hypotheses assume rampant hybridization of *R. tagoi* A-2 and *R. sakurii* in the
364 past. The IM analyses based on two different models showed gene flow from *R. tagoi* to *R.*
365 *sakurii*. However, this unidirectional gene flow seems to depend largely on the flow from *R.*
366 *tagoi* A-5+6 to *R. sakurii*, because no significant flow between *R. tagoi* A-2 and *R. sakurii*
367 was detected (Table 2). These results do not support rampant hybridization of *R. tagoi* A-2 and
368 *R. sakurii*, even though inter-specific gene flow did exist. From these considerations, the ILS
369 hypothesis would be more plausible than the introgression hypothesis to explain the
370 relationships of the two species on the mitochondrial genealogy.

371 The estimated time of the split of *R. sakurii* and *R. tagoi* Lineage A-2 (ca. 1.2–1.1 MYA) is
372 younger than those of other Japanese frogs (e.g., ca. 2.3 MYA between *Odorrana ishikawae/O.*
373 *splendida* and ca. 1.7 MYA between *O. amamiensis/O. narina* [Matsui et al., 2005]; and around
374 5.7–4.0 MYA among *Bufo torrenticola* and two subspecies of *B. japonicus* [Igawa et al., 2006]),
375 and seems to have occurred after the rough formation of the Japanese archipelago (see the next
376 section). Although the ILS of mtDNA at the species level is relatively rare because of its small
377 effective number of gene copies, it occurs occasionally in some situations, such as speciation
378 within the past millions years. It could be applicable in the case of *R. sakurii* and *R. tagoi*,
379 because their speciation is estimated to be only about one million year ago. *Rana sakurii* has
380 several traits adaptive to stream breeding in contrast to the subterranean breeding *R. tagoi*,
381 although they share many other characters (Matsui and Matsui, 1990). It suggests that the
382 speciation of *R. sakurii* was triggered by adaptation to a new breeding habitat, which is a
383 process that often promotes rapid speciation (Coyne and Orr, 2004).

384 4.2. Evolutionary history of the two species

385 *Rana tagoi* and *R. sakurii* are endemic to the Japanese archipelago and no close relatives
386 are known from the continent, although *R. sauteri*, a lotic breeding brown frog from Taiwan, is
387 thought to be their sister lineage (Tanaka-Ueno et al., 1998). Our data do not contradict with this
388 idea (Fig. 1). Since the continental allies of *R. sauteri* are also unknown, the dispersal route of

389 the ancestor of the *R. tagoi* complex to the Japanese mainland is uncertain. The estimated time
390 of separation of *R. sauteri* and *R. tagoi* complex varies between the calibrations (22.0–11.6
391 MYA; Table 1), but around the early to middle Miocene. In this period the opening of the Japan
392 Sea began (Iijima and Tada, 1990), although the Japanese and Ryukyu archipelagos, as well as
393 Taiwan were not yet isolated from the Eurasian continent (Chinzei and Machida, 2001).
394 Therefore the common ancestor of *R. sauteri* and the *R. tagoi* complex would have been
395 distributed in the continental areas corresponding to the present Japanese archipelago to Taiwan,
396 but the ancestral allies would have been extinguished thereafter on the continent and the
397 Ryukyus, leaving relict species in Japan and Taiwan.

398 In any case, the ancestral population of the *R. tagoi* complex is thought to have diverged
399 into two major clades, A and B (Fig. 2), in the mid Pliocene (ca. 4.2–4.0 MYA). The ancient
400 Japanese archipelago was already roughly formed by the late Miocene (Chinzei and Machida,
401 2001), and the separation of lineages ancestral to the clades is thought to have occurred on the
402 archipelago. The ancestor at this period would have been a *R. tagoi*-like subterranean breeder
403 because all of the present genetic groups of the two species have a common larval trait (e.g., no
404 need to feed until metamorphosis) thought to be adapted to such an environment.

405 Then, the divergence within Clade A occurred in the late Pliocene (ca. 2.8–2.6 MYA),
406 separating populations on or near Honshu from ones on or near from Kyushu and Shikoku.
407 Cluster II as identified by nuclear markers (Fig. 3) is equivalent to populations diagnosed by
408 mitochondrial haplotype Subclade A' excluding Lineage A-1a. Lineages of Subclade A' occur
409 on Honshu, whereas those of mitochondrial Subclade A'' are associated with Kyushu or Shikoku.
410 Because populations of mitochondrial haplotype Clade B also occur on Honshu, Honshu is
411 likely the ancestral source of this species complex, and expansion to the ancestral areas of
412 Kyushu and Shikoku likely produced the major cladogenetic event within mitochondrial Clade
413 A. Approximately 1.8–1.4 MYA (the divergence time estimated for mitochondrial haplotypes
414 of Lineages A-1a and A-1b), introgression of mitochondrial haplotypes from a population in

415 mitochondrial Subclade A' to one in Clade B produced the anomalous result that Lineage A-1a
416 appears in an incorrect position on the mitochondrial haplotype tree. The best interpretation is
417 that Lineage A-1a is closest phylogenetically to the lineages of mitochondrial Clade B as
418 revealed by the nuclear markers, in contrast to its position on the mitochondrial haplotype tree.
419 Occurrence of Subclade A' and Clade B in geographic proximity on Honshu further supports
420 this interpretation. The divergences within Subclades A', A'', and Clade B started around 2.7–2.3
421 MYA, and splitting of the major mt-lineages was roughly completed by the middle Pleistocene
422 (around 1.4 MYA). In this period, the populations on peripheral islands were isolated
423 geographically, and some survived and evolved into the extant subspecies; *i.e.*, *R. t.*
424 *yakushimensis* of Lineage A-8 and *R. t. okiensis* of B-1.

425 The estimated date of speciation of *R. sakuraii* was younger than the formation of the major
426 population lineages discussed above. *Rana sakuraii* would have originated ca. 1.2–1.1 MYA
427 based on the IM analysis (Table 2), likely in association with the adaptation to a new breeding
428 environment as discussed above. The effective population size of *R. sakuraii* (ca. 0.2 million
429 individuals) is smaller than that of the closest mt-lineage of *R. tagoi* (ca. 0.8 million individuals
430 for Lineage A-2), and suggests that a small ancestral population adapted to stream breeding led
431 to *R. sakuraii*.

432

433 **5. Conclusion**

434 Our data reveal that *R. tagoi* comprises multiple species lineages, which form a paraphyletic
435 group with respect to *R. sakuraii*. Because *R. sakuraii* arose only about one million years ago,
436 incomplete lineage sorting of mitochondrial haplotypes best explains non-monophyly of *R.*
437 *sakuraii* on the mitochondrial haplotype tree. Our study illustrates how mitochondrial haplotype
438 phylogenies combined with multilocus demographic analyses of nuclear haplotypes permits
439 precise resolution of species lineages and their genetic interactions.

440

441 **Acknowledgements**

442 We would like to thank G. Aoki, K. Araya, H. Fujita, T. Hayashi, A. Hamidy, T. Hikida, M.
443 Kato, Y. Kawahara, K. Kawauchi, Y. Kokuryo, N. Kuraishi, N. Maeda, Mm, Matsui, T. Matsuki,
444 T. Matsuo, Y. Misawa, Y. Miyagata, A. Mori, S. Mori, N. Nakahama, T. Nakano, Y. Nakase, K.
445 Nishikawa, S. Okada, J. Oki, M. Sakamoto, T. Shimada, T. Sugahara, T. Sugihara, H. Takeuchi,
446 S. Tanabe, A. Tominaga, T. Ueno, M. Yamagami, Y. Yamane, Y. Yamazaki, N. Yoshikawa,
447 and everyone else who helped us in collecting specimens. KE thanks N. Kuraishi and N.
448 Yoshikawa for assisting laboratory works. We are also grateful to A. Larson and anonymous
449 reviewers for valuable comments on the manuscript. This work was partly supported by grants
450 from the Ministry of Education, Science and Culture, Japan (Nos. 07454234, 20405013 and
451 23405014) to MM.

452

453 **References**

- 454 Ballard, J.W.O., Whitlock, M.C., 2004. The incomplete natural history of mitochondria. *Mol.*
455 *Ecol.* 13, 729–744.
- 456 Bandelt, H., Forster, P., Röhl, A., 1999. Median-joining networks for inferring intraspecific
457 phylogenies. *Mol. Biol. Evol.* 16, 37–48.
- 458 Chinzei, K., Machida, H., 2001. Formation history of structural landforms and tectonic
459 landforms in Japan, in: Yonekura, N., Kaizuka, S., Nogami, M., Chinzei, K. (Eds.),
460 *Regional Geomorphology of the Japanese Islands, Introduction to Japanese*
461 *Geomorphology*, Vol. 1. University of Tokyo Press, Tokyo, pp. 298–311.
- 462 Coyne, J.A., Orr, H.A., 2004. *Speciation*. Sinauer Associates, Sunderland, MA.
- 463 Drummond, A.J., Suchard, M.A., Xie, D., Rambaut, A., 2012. Bayesian phylogenetics with
464 BEAUti and the BEAST 1.7. *Mol. Biol. Evol.* 29, 1969–1973.
- 465 Edgar, R., 2004. MUSCLE: multiple sequence alignment with high accuracy and high
466 throughput. *Nucleic Acids Res.* 32, 1792–1797.

- 467 Eto, K., Matsui, M., Sugahara, T., 2013. Discordance between mitochondrial DNA genealogy
468 and nuclear DNA genetic structure in the two morphotypes of *Rana tagoi tagoi*
469 (Amphibia: Anura: Ranidae) in the Kinki Region, Japan. *Zool. Sci.* 30, 553–558.
- 470 Eto, K., Matsui, M., Sugahara, T., Tanaka-Ueno, T., 2012. Highly complex mitochondrial DNA
471 genealogy in an endemic Japanese subterranean breeding brown frog *Rana tagoi*
472 (Amphibia, Anura, Ranidae). *Zool. Sci.* 29, 662–671.
- 473 Evanno, G., Regnaut, S., Goudet, J., 2005. Detecting the number of clusters of individuals using
474 the software STRUCTURE: a simulation study. *Mol. Ecol.* 14, 2611–2620.
- 475 Fouquet, A., Green, D.M., Waldman, B., Bowsher, J.H., McBride, K.P., Gemmell, N.J., 2010.
476 Phylogeography of *Leiopelma hochstetteri* reveals strong genetic structure and suggests
477 new conservation priorities. *Conserv. Genet.* 11, 907–919.
- 478 Garrick, R.C., Sunnucks, P., Dyer, R.J., 2010. Nuclear gene phylogeography using PHASE:
479 dealing with unresolved genotypes, lost alleles, and systematic bias in parameter
480 estimation. *BMC Evol. Biol.* 10, 118.
- 481 Hey, J., 2010. Isolation with migration models for more than two populations. *Mol. Biol. Evol.*
482 27, 905–920.
- 483 Hey, J., Nielsen, R., 2004. Multilocus methods for estimating population sizes, migration rates
484 and divergence time, with applications to the divergence of *Drosophila pseudoobscura* and
485 *D. persimilis*. *Genetics* 167, 747–760.
- 486 Hurt, C., Silliman, K., Anker, A., Knowlton, N., 2013. Ecological speciation in anemone-
487 associated snapping shrimps (*Alpheus armatus* species complex). *Mol. Ecol.* 22, 4532–
488 4548.
- 489 Igawa, T., Kurabayashi, A., Nishioka, M., Sumida, M., 2006. Molecular phylogenetic
490 relationship of toads distributed in the Far East and Europe inferred from the nucleotide
491 sequences of mitochondrial DNA genes. *Mol. Phylogenet. Evol.* 38, 250–260.

492 Iijima, A., Tada, R., 1990. Evolution of tertiary sedimentary basins of Japan in reference to
493 opening of the Japan Sea. J. Fac. Sci. Univ. Tokyo, Sect. II 22, 121–171.

494 Jacobsen, F., Omland, K.E., 2012. Extensive introgressive hybridization within the northern
495 oriole group (Genus *Icterus*) revealed by three-species isolation with migration analysis.
496 Ecol. Evol. 2, 2413–2429.

497 Jobb, G., 2011. TREEFINDER version March 2011. <<http://www.treefinder.de>>.

498 Kusano, T., Fukuyama, K., Miyashita, N., 1995a. Age determination of the stream frog, *Rana*
499 *sakuraii*, by skeletochronology. J. Herpetol. 29, 625–628.

500 Kusano, T., Fukuyama, K., Miyashita, N., 1995b. Body size and age determination brown frog
501 *Rana tagoi tagoi* by skeletochronology in southwestern Kanto. Jpn. J. Herpetol. 16, 29–34.

502 Lawson, L.P., 2010. The discordance of diversification: evolution in the tropical-montane frogs
503 of the Eastern Arc Mountains of Tanzania. Mol. Ecol. 19, 4046–4060.

504 Macey, J.R., Schulte, J.A., Larson, A., Fang, Z., Wang, Y., Tuniyev, B.S., Papenfuss, T.J., 1998.
505 Phylogenetic relationships of toads in the *Bufo bufo* species group from the eastern
506 escarpment of the Tibetan Plateau: a case of vicariance and dispersal. Mol. Phylogenet.
507 Evol. 9, 80–87.

508 Macey, J.R., Strasburg, J.L., Brisson, J. a, Vredenburg, V.T., Jennings, M., Larson, A., 2001.
509 Molecular phylogenetics of western North American frogs of the *Rana boylei* species
510 group. Mol. Phylogenet. Evol. 19, 131–143.

511 Maeda, N., Matsui, M., 1999. Frogs and Toads of Japan, Revised Edition. Bun-ichi Sogo
512 Shuppan, Tokyo.

513 Matsui, M., 2011. On the brown frogs from the Ryukyu Archipelago, Japan, with descriptions
514 of two new species (Amphibia, Anura). Curr. Herpetol. 30, 111–128.

515 Matsui, M., Shimada, T., Ota, H., Tanaka-Ueno, T., 2005. Multiple invasions of the Ryukyu
516 Archipelago by Oriental frogs of the subgenus *Odorrana* with phylogenetic reassessment
517 of the related subgenera of the genus *Rana*. Mol. Phylogenet. Evol. 37, 733–742.

518 Matsui, T., Matsui, M., 1990. A new brown frog (genus *Rana*) from Honshu, Japan.
519 Herpetologica 46, 78–85.

520 Mitsui, Y., Setoguchi, H., 2012. Demographic histories of adaptively diverged riparian and non-
521 riparian species of *Ainsliaea* (Asteraceae) inferred from coalescent analyses using multiple.
522 BMC Evol. Biol. 12, 254.

523 Nielsen, R., Wakeley, J., 2001. Distinguishing migration from isolation: a Markov chain Monte
524 Carlo approach. Genetics 158, 885–896.

525 Pritchard, J., Stephens, M., Donnelly, P., 2000. Inference of population structure using
526 multilocus genotype data. Genetics 155, 945–959.

527 Rambaut, A., Drummond, A., 2009. Tracer version 1.5. <<http://beast.bio.ed.ac.uk/Tracer>>.

528 Reilly, S.B., Marks, S.B., Jennings, W.B., 2012. Defining evolutionary boundaries across
529 parapatric ecomorphs of Black Salamanders (*Aneides flavipunctatus*) with conservation
530 implications. Mol. Ecol. 21, 5745–5761.

531 Roelants, K., Gower, D.J., Wilkinson, M., Loader, S.P., Biju, S.D., Guillaume, K., Moriau, L.,
532 Bossuyt, F., 2007. Global patterns of diversification in the history of modern amphibians.
533 Proc. Natl. Acad. Sci. U. S. A. 104, 887–892.

534 Ronquist, F., Huelsenbeck, J.P., 2003. MrBayes 3: Bayesian phylogenetic inference under
535 mixed models. Bioinformatics 19, 1572–1574.

536 Rovito, S.M., 2010. Lineage divergence and speciation in the Web-toed Salamanders
537 (Plethodontidae: *Hydromantes*) of the Sierra Nevada, California. Mol. Ecol. 19, 4554–
538 4571.

539 Rozas, J., Sanchez-DelBarrio, J.C., Messeguer, X., Rozas, R., 2003. DnaSP, DNA
540 polymorphism analyses by the coalescent and other methods. Bioinformatics 19, 2496–
541 2497.

542 Stephens, M., Smith, N., Donnelly, P., 2001. A new statistical method for haplotype
543 reconstruction from population data. Am. J. Hum. Genet. 68, 978–989.

- 544 Tajima, F., 1989. Statistical method for testing the neutral mutation hypothesis by DNA
545 polymorphism. *Genetics* 123, 585–595.
- 546 Tanabe, A.S., 2011. Kakusan4 and Aminosan: two programs for comparing nonpartitioned,
547 proportional and separate models for combined molecular phylogenetic analyses of
548 multilocus sequence data. *Mol. Ecol. Resour.* 11, 914–921.
- 549 Tanaka, T., Matsui, M., Takenaka, O., 1996. Phylogenetic relationships of Japanese brown
550 frogs (*Rana*: Ranidae) assessed by mitochondrial cytochrome b gene sequences. *Biochem.*
551 *Syst. Ecol.* 24, 299–307.
- 552 Tanaka-Ueno, T., Matsui, M., Chen, S.-L., Takenaka, O., Ota, H., 1998. Phylogenetic
553 relationships of brown frogs from Taiwan and Japan assessed by mitochondrial
554 cytochrome b gene sequences (*Rana*: Ranidae). *Zool. Sci.* 15, 283–288.
- 555 Tavaré, S., 1986. Some probabilistic and statistical problems in the analysis of DNA sequences,
556 in: Miura, R.M. (Ed.), *Lectures on Mathematics in the Life Sciences*. pp. 57–86.
- 557 Waples, R., Gaggiotti, O., 2006. What is a population? An empirical evaluation of some genetic
558 methods for identifying the number of gene pools and their degree of connectivity. *Mol.*
559 *Ecol.* 15, 1419–1439.
- 560 Woerner, A.E., Cox, M.P., Hammer, M.F., 2007. Recombination-filtered genomic datasets by
561 information maximization. *Bioinformatics* 23, 1851–1853.
- 562 Wright, S., 1931. Evolution in Mendelian populations. *Genetics* 16, 97–159.

563

564 **Supporting information**

565 Additional supporting information may be found in the online version of this article.

566

567 **Table Captions**

568 **Table 1** The mean estimated divergence times (MYA) for *R. tagoi*, *R. sakurii*, and the
569 outgroups. Values in parentheses are the 95% highest posterior density interval. For the node
570 numbers, refer to Fig. 2.

571

572 **Table 2** Demographic parameters estimated in the IM analysis. N_e , effective population size
573 (million individuals); $2N_eM$, effective population migration rate (number of gene
574 copies/generation), for which $2N_eM_{1\rightarrow 2}$ ($2N_eM_{2\rightarrow 1}$) indicates gene flow from group 1 to 2 (2 to
575 1) forwards in time; T , population divergence time (MYA). Values supported by the highest
576 probability are shown as HiPt, and HPD95 indicates the 95% highest posterior density interval.
577 Parameters in bold indicate the values with statistical support, and characters in italics are those
578 with no significant peak of posterior probability density.

579

580 **Figure Captions**

581 **Fig. 1** Map showing the sampling localities of *Rana tagoi tagoi* (circles), *R. t. yakushimensis*
582 (double circle), *R. t. okiensis* (stars), and *R. sakurii* (triangles). Each species lineage inferred
583 using mitochondrial haplotypes is represented by different markers. For the locality information,
584 see Table S1.

585

586 **Fig. 2** Maximum-likelihood tree based on the complete mitochondrial *16S* and *ND1* sequences
587 (2579 bp in total) for *Rana tagoi* and *R. sakurii*. For the locality number, see Fig. 1.
588 Haplotypes in Clades A' and B are sampled from Honshu or the Oki Island (B-1). Haplotypes in
589 Clades A'' are from Kyushu, Shikoku, or adjacent small islands.

590

591 **Fig. 3** Results of STRUCTURE analyses based on the five nuclear genes. Each species lineage
592 inferred using mitochondrial haplotypes is separated by black vertical lines. (top) The best

593 clustering result ($K = 2$ clusters) for all 128 samples. (left bottom) Results with $K=2$ (best) and 3
594 for Cluster I. (right bottom) Results with $K=3$ (best) and 4 for Cluster II.

595

596 **Fig. 4** Hypothesized scenarios for non-monophyly of mitochondrial haplotypes in *R. sakurarii*:
597 (1) the species-level ILS hypothesis; and (2) the past mitochondrial introgression hypothesis, in
598 which introgression occurred from *R. tagoi* Lineage A-2 to *R. sakurarii* (a) or in the opposite
599 direction (b). Solid and broken lines indicate the mitochondrial lineages of *R. tagoi* and *R.*
600 *sakurarii*, respectively. Grey arrows indicate massive mitochondrial introgression.

601

602 **Captions for supplementary materials**

603 **Table S1** The samples used in this study with information on the sampling localities, vouchers,
604 and GenBank accession numbers for each locus. KUHE, Graduate School of Human and
605 Environmental Studies, Kyoto University; TMP, temporary number.

606

607 **Table S2** The primers used to amplify mt- and n-DNA in this study.

608

609 **Table S3** Summary statistics of each locus. Tajima's D values; length of sequence after
610 alignment; variable sites (vs); number of haplotypes (h); haplotype diversity (Hd); and
611 nucleotide diversity (π).

612

613 **Fig. S1** Median-joining networks of five nuclear loci. The size of each circle reflects the relative
614 sample size of each haplotype. The color indicates nuclear clusters and species as follows: red =
615 n-Cluster I of *R. tagoi*; green = n-Cluster II of *R. tagoi*; light green = n-Cluster II of *R. sakurarii*.
616 Black circles and bars indicate median vectors and missing haplotypes, respectively.

617

618 **Fig. S2** Posterior probability densities for divergence time (T), effective population size (N_e),
619 and population migration rate ($2N_eM$) of Clusters I and II obtained in the IM analyses. The
620 resultant values and 95% confidence intervals for each estimate are listed in Table 2.

621

622 **Fig. S3** Posterior probability densities for divergence time (T , left top), effective population size
623 (N_e , left middle and bottom), and population migration rate ($2N_eM$, right) of *R. tagoi* (R_t)
624 lineage A-2, A-5+6, and *R. sakurarii* (R_s). Estimates with no statistical support are indicated by
625 *ns*. The parameters obtained in three- and two-populations models are shown as triangles and
626 circles, respectively. The resultant values and 95% confidence intervals for each estimate are
627 listed in Table 2.

628

629

630 The English in this document has been checked by at least two professional editors, both native
631 speakers of English. For a certificate, please see:

632 <http://www.textcheck.com/>

633 certificate/wc1m0N

634

Table 1 The mean estimated divergence times (MYA) for *R. tagoi*, *R. sakurarii*, and the outgroups. Values in parentheses are the 95% highest posterior density interval. For the node numbers, refer to Fig.

Node	Calibration I	Calibration II
1	4.00 (5.96–2.33)	4.16 (6.16–2.44)
2	2.58 (3.82–1.60)	2.82 (4.07–1.69)
3	2.31 (3.38–1.42)	2.46 (3.54–1.45)
4	1.84 (2.69–1.05)	1.73 (2.60–0.99)
5	1.16 (1.87–0.60)	1.04 (1.66–0.50)
6	1.32 (2.00–0.69)	1.35 (2.06–0.70)
7	1.87 (2.78–1.05)	2.08 (3.07–1.21)
8	0.95 (1.60–0.44)	1.13 (1.78–0.58)
9	0.88 (1.40–0.41)	1.39 (2.16–0.72)
10	1.92 (2.85–1.09)	2.12 (3.14–1.24)
11	1.75 (2.59–0.96)	1.69 (2.50–0.90)
12	0.50 (0.95–0.14)	0.42 (0.81–0.11)
13	1.15 (1.85–0.56)	1.50 (2.30–0.82)
14	0.36 (0.64–0.13)	0.53 (0.90–0.21)
15	2.31 (3.36–1.34)	2.54 (3.70–1.53)
16	0.79 (1.30–0.34)	0.85 (1.38–0.37)
17	0.20 (0.43–0.03)	0.17 (0.37–0.01)
18	1.68 (2.53–0.99)	1.98 (2.91–1.19)
19	0.53 (0.90–0.21)	0.59 (1.01–0.24)
20	1.04 (1.67–0.46)	1.40 (2.11–0.73)
21	1.46 (2.22–0.76)	1.54 (2.34–0.83)
22	2.71 (4.34–1.40)	2.29 (3.50–1.24)
23	1.40 (2.15–0.71)	1.35 (2.07–0.71)
24	0.80 (1.28–0.36)	0.82 (1.32–0.39)
25	0.90 (1.46–0.42)	1.08 (1.74–0.52)
26	0.04 (0.13–0.03)	0.26 (0.53–0.05)
O-1	22.02 (35.97–11.08)	11.59 (18.29–6.42)

Table 2 Demographic parameters estimated in the IM analysis. N_e , effective population size (million individuals); $2N_eM$, effective population migration rate (number of gene copies/generation), for which $2N_eM_{1 \rightarrow 2}$ ($2N_eM_{2 \rightarrow 1}$) indicates gene flow from group 1 to 2 (2 to 1) forwards in time; T , population divergence time (MYA). Values supported by the highest probability are shown as HiPt, and HPD95 indicates the 95% highest posterior density interval. Parameters in bold indicate the values with statistical support and characters in italics are those with no significant peak of posterior probability density.

	N_1	N_2	N_{ancestor}	$2N_eM_{1 \rightarrow 2}$	$2N_eM_{2 \rightarrow 1}$	T
(1) Cluster I vs. (2) Cluster II						
HiPt	2.18	1.73	0.40	0.52	1.23	2.72
HPD95	(1.70–2.87)	(1.34–2.30)	(0.17–0.79)	(0.24–1.12)	(0.70–2.14)	(2.10–4.29)
Three-pops. model: (1) <i>R. sakurarii</i> vs. (2) <i>R. tagoi</i> lin						
HiPt	0.16	0.80	0.21	0.01	0.00	1.05
HPD95	(0.07–0.32)	(0.34–2.06)	(0.01–4.06)	(0.00–2.46)	(0.00–0.84)	(0.63–2.26)
Three-pops. model: (1) <i>R. sakurarii</i> vs. (2) <i>R. tagoi</i> lineage A-5, 6						
HiPt	0.16	0.79	-	0.46	0.40	-
HPD95	(0.07–0.31)	(0.38–1.76)	-	(0.00–2.52)	(0.04–2.00)	-
Three-pops. model: (1) <i>R. tagoi</i> A-2 vs. (2) <i>R. tagoi</i> A-5, 6						
HiPt	0.80	0.79	-	0.17	3.79	-
HPD95	(0.34–2.06)	(0.38–1.76)	-	(0.00–3.74)	(0.75–9.50)	-
Three-pops. model: (1) ancestor of <i>R. sakurarii</i> and <i>R. tagoi</i> A-2 vs. (2) <i>R. tagoi</i> A-5, 6						
HiPt	0.21	0.79	0.43	<i>0.06</i>	<i>0.04</i>	2.15
HPD95	(0.01–4.06)	(0.38–1.76)	(0.23–0.77)	(0.00–81.15)	(0.00–34.07)	(1.31–6.11)
Two-pops. model: (1) <i>R. sakurarii</i> vs. (2) <i>R. tagoi</i> A-2, 5, 6						
HiPt	0.17	1.61	0.37	0.01	0.51	1.21
HPD95	(0.09–0.34)	(0.99–2.65)	(0.10–0.68)	(0.00–3.19)	(0.14–1.17)	(0.56–2.85)

64 Toyo Town, Kochi Pref.	29464	A-7	AB639510, AB639679	AB968675	AB968804	AB968930	AB969059	AB969188
65 Saijo City, Ehime Pref.	27679	A-7	AB639507, AB639676	AB968672	AB968802	AB968928	AB969057	AB969185
	43078	A-7	AB968264	AB968712	AB968841	AB968967	AB969096	AB969224
66 Saiyo City, Ehime Pref.	TMP_T2241	A-7	AB639509, AB639678	AB968769	AB968897	AB969023	AB969152	AB969282
67 Kitakyushu City, Fukuoka Pref.	28612	A-9a	AB968255	AB968674	AB968798	AB968924	AB969053	AB969187
68 Beppu City, Oita Pref.	43637	A-9a	AB639519, AB639688	AB968723	AB968852	AB968978	AB969107	AB969235
69 Yatsushiro City, Kumamoto Pref.	27562	A-9a	AB639524, AB639691	AB968668	AB968797	AB968923	AB969052	AB969181
70 Amakusa City, Kumamoto Pref.	30342	A-9a	AB639525, AB639692	AB968679	AB968808	AB968934	AB969063	AB969192
71 Kanoya City, Kagishima Pref.	27295	A-9a	AB639530, AB639697	AB968664	AB968793	AB968919	AB969048	AB969177
72 Sasebo City, Nagasaki Pref.	27140	A-9a	AB639518, AB639687	AB968663	AB968792	AB968918	AB969047	AB969176
73 Goto City, Nagasaki Pref.	45359	A-9a	AB968295	AB968754	AB968883	AB969010	AB969139	AB969267
	45362	A-9a	AB968296	AB968755	AB968884	AB969011	AB969140	AB969268
74 Nobeoka City, Miyazaki Pref.	27121	A-9b	AB639528, AB639695	AB968662	AB968791	AB968917	AB969046	AB969175
75 Nishimera Village, Miyazaki Pref.	26088	A-9b	AB639529, AB639696	AB968661	AB968790	AB968916	AB969045	AB969174
76 Miyakonojo City, Miyazaki Pref.	30907	A-9b	AB639532, AB639699	AB968680	AB968809	AB968935	AB969064	AB969193
77 Kimotsuki City, Kagoshima Pref.	43397	A-9b	AB639533, AB639700	AB968714	AB968843	AB968969	AB969098	AB969226
78 Kinko Town, Kagoshima Pref.	27678	A-9b	AB639536, AB639703	AB968671	AB968801	AB968927	AB969056	AB969184
79 Goto City, Nagasaki Pref.	31539	A-9c	AB639538, AB639705	AB968681	AB968810	AB968936	AB969065	AB969194
79 Shinkamigoto City, Nagasaki Pref.	45149	A-9c	AB968291	AB968750	AB968879	AB969006	AB969135	AB969263
	TMP_110216-1	A-9c	AB968252	AB968650	AB968774	AB968906	AB969034	AB969163
80 Goto City, Nagasaki Pref.	44316	A-9c	AB968278	AB968736	AB968866	AB968991	AB969120	AB969248
	44317	A-9c	AB968279	AB968737	AB968867	AB968992	AB969121	AB969249
	45355	A-9c	AB968294	AB968753	AB968882	AB969009	AB969138	AB969266
<i>R. t. okiensis</i>								
50 Okinoshima Town, Shimane Pref.	10818	B-1	AB639576, AB639742	AB968649	AB968778	AB968905	AB969033	AB969162
	22341	B-1	AB639579, AB639742	AB968656	AB968785	AB968911	AB969040	AB969169
51 Nishinoshima Town, Shimane Pref.	43647	B-1	AB639580, AB639742	AB968724	AB968853	AB968979	AB969108	AB969236
<i>R. t. yakushimensis</i>								
81 Yakushima Town, Kagoshima Pref.	10182	A-8	AB639578, AB639741	AB968646	AB968775	AB968902	AB969030	AB969159
	45177	A-8	AB968292	AB968751	AB968880	AB969007	AB969136	AB969264
	45182	A-8	AB968293	AB968752	AB968881	AB969008	AB969137	AB969265
<i>R. sakuraii</i>								
11 Kanuma City, Tochigi Pref.	43633	A-2	AB968268	AB968720	AB968849	AB968975	AB969104	AB969232
	43634	A-2	AB968269	AB968721	AB968850	AB968976	AB969105	AB969233
	43635	A-2	AB639423, AB639744	AB968722	AB968851	AB968977	AB969106	AB969234
15 Akiruno City, Tokyo Pref.	42450	A-2	AB639583, AB639744	AB968704	AB968833	AB968959	AB969088	AB969216
	43740	A-2	AB968271	AB968726	AB968855	AB968981	AB969110	AB969238
17 Minobu Town, Yamanashi Pref.	45620	A-2	AB968301	AB968760	AB968889	AB969016	AB969145	AB969273
20 Shizuoka City, Shizuoka Pref.	unnumbered	A-2	AB639488, AB639749	AB968766	AB968900	AB969022	AB969151	AB969280
	44254	A-3	AB968275	AB968733	AB968862	AB968988	AB969117	AB969246
	44286	A-3	AB968277	AB968735	AB968865	AB968990	AB969119	AB969247
21 Shizuoka City, Shizuoka Pref.	44256	A-2	AB968276	AB968734	AB968863	AB968989	AB969118	AB969245
22 Matsumoto City, Nagano Pref.	22887	A-2	AB639585, AB639746	AB968657	AB968786	AB968912	AB969041	AB969170
24 Kurobe City, Toyama Pref.	45105	A-3	AB968289	AB968748	AB968878	AB969004	AB969133	AB969261
24 Kurobe City, Toyama Pref.	45106	A-3	AB968290	AB968749	AB968864	AB969005	AB969134	AB969262
32 Katsuyama City, Fukui Pref.	43591	A-3	AB968267	AB968719	AB968848	AB968974	AB969103	AB969231
38 Odai Town, Mie Pref.	27647	A-3	AB639554, AB639719	AB968669	AB968799	AB968925	AB969054	AB969182
	40309	A-3	AB639555, AB639720	AB968692	AB968821	AB968947	AB969076	AB969204
	45049	A-3	AB968285	AB968744	AB968874	AB969000	AB969129	AB969256
41 Nantan City, Kyoto Pref.	41412	A-3	AB639455, AB639632	AB968696	AB968825	AB968951	AB969080	AB969208
	unnumbered	A-3	AB639454, AB639631	AB968767	AB968895	AB969026	AB969155	AB969285
48 Wakasa Town, Tottori Pref.	34740	A-3	AB968257	AB968683	AB968812	AB968938	AB969067	AB969195
59 Iwakuni City, Yamaguchi Pref.	43893	A-3	AB639590, AB639750	AB968729	AB968858	AB968984	AB969113	AB969241
<i>R. tsushimensis</i>								
Tsushima City, Nagasaki Pref.	10606		AB639592, AB639752	-	-	-	-	-
<i>R. kobai</i>								
Amami City, Kagoshima Pref.	10051		AB685768	-	-	-	-	-
<i>R. ulma</i>								
Higashi Village, Okinawa Pref.	10056		AB685780	-	-	-	-	-
<i>R. sauteri</i>								
Chiayi County, Taiwan	6894		AB685767	-	-	-	-	-

Table S2 The primers used to amplify mt- and n-DNA in this study.

Target	Name	Sequence	Reference
<i>16S</i>	L1507	TACACACCGCCCGTCACCCCTCTT	Shimada et al (2011)
	H1923	AAGTAGCTCGCTTAGTTTCGG	Shimada et al (2011)
	L1879	CGTACCTTTTGCATCATGGTC	Shimada et al (2011)
	H2315	TTCTTGTTACTAGTTCTAGCAT	Shimada et al (2011)
	L2188	AAAGTGGGCTAAAAGCAGCCA	Matsui et al (2006)
	Wilkinson_6	CCCTCGTGATGCCGTTGATAC	Wilkinson et al (2002)
	16L1	CTGACCGTGCAAAGGTAGCGTAATCACT	Hedges (1994)
<i>ND1</i>	16H1	CTCCGGTCTGAACTCAGATCACGTAGG	Hedges (1994)
	L3032	CGACCTCGATGTTGGATCAGG	Shimada et al (2011)
	ND1_Htago	GRGCRATTTGGAGTTTGARGCTCA	Eto et al (2012)
	ND1_Ltago	GACCTAAACCTCAGYATYCTATTTAT	Eto et al (2012)
	tMet_H	AGGAAGTACAAAAGGTTTGTATC	Shimada et al (2011)
<i>NCX1</i>	NCX1F	ACAACAGTRAGRATATGGAA	Shimada et al. (2011)
	NCX1R1	GCCATATCTCTCCTCGCTTCTTC	Eto et al (2013)
<i>NF1A</i>	NF1A-005_F	FTTTGTACATCAGGTGTTTT	This study
	NF1A-005_R	CTTGCCCTGGCTGCT	This study
<i>POMC</i>	POMC1	GAATGTATYAAAGMMTGCAAGATGGWCC	Wiens et al. (2005)
	POMC7	TGGCATTTTGAAAAGAGTCAT	Smith et al. (2005)
<i>SLC8A3</i>	SCF_2F	CAAACACAGRGSAAATTATGAT	Shimada et al (2011)
	SCF_2R	ATAATYCCAACCTGARAACCTC	Shimada et al (2011)
<i>TYR</i>	Tyr_L1	CCCCAGTGGGYRCCCARTTCCC	Kuraishi et al (2013)
	Tyr_H1	CCACCTTCTGGATTCCCGTTC	Kuraishi et al (2013)

References

- Eto, K., Matsui, M., Sugahara, T., 2013. Discordance between mitochondrial DNA genealogy and nuclear DNA genetic structure in the two morphotypes of *Rana tagoi tagoi* (Amphibia: Anura: Ranidae) in the Kinki Region, Japan. *Zool. Sci.* 30, 553–558.
- Eto, K., Matsui, M., Sugahara, T., Tanaka-Ueno, T., 2012. Highly complex mitochondrial DNA genealogy in an endemic Japanese subterranean breeding brown frog *Rana tagoi* (Amphibia, Anura, Ranidae). *Zool. Sci.* 29, 662–671.
- Kuraishi, N., Matsui, M., Hamidy, A., Belabut, D.M., Ahmad, N., Panha, S., Sudin, A., Yong, H.S., Jiang, J.-P., Ota, H., Thong, H.T., Nishikawa, K., 2013. Phylogenetic and taxonomic relationships of the *Polypedates leucomystax* complex (Amphibia). *Zool. Scripta*, 42, 54–70.
- Matsui M, Shimada T, Liu W.-Z., Maryati, M., Khonsue, W., Orlov, N., 2006. Phylogenetic relationships of Oriental torrent frogs in the genus *Amolops* and its allies (Amphibia, Anura, Ranidae). *Mol. Phylogenet. Evol.* 38, 659–666.
- Shimada, T., Matsui, M., Yambun, P., Sudin, A. 2011. A taxonomic study of Whitehead's torrent frog, *Meristogenys whiteheadi*, with descriptions of two new species (Amphibia: Ranidae). *Zool. J. Linnean. Soc.* 161, 157–183.
- Smith, S.A., Stephens, P.R., Wiens, J., 2005. Replicate patterns of species richness, historical biogeography, and phylogeny in Holarctic treefrogs. *Evolution*, 59, 2433–2450.
- Wiens, J., Fetzner, J.W. Jr, Parkinson, C.L., Reeder, T.W., 2005. Hylid frog phylogeny and sampling strategies for species clades. *Syst. Biol.* 54, 719–748.
- Wilkinson, J.A., Drewes, R.C., Tatum, O.L., 2002. A molecular phylogenetic analysis of the family Rhacophoridae with an emphasis on the Asian and African genera. *Mol. Phylogenet. Evol.* 24, 265–273.

Table S3 Summary statistics of each locus. Tajima's D values; length of sequence after alignment; variable sites (vs); number of haplotypes (h); haplotype diversity (Hd); and nucleotide diversity (π).

	Tajima's L sites						vs				h				Hd				π			
	vs	h	Hd	π	vs	h	Hd	π	vs	h	Hd	π	vs	h	Hd	π	vs	h	Hd	π		
	whole (n = 128)						mt-lineage A-1a (n = 18)				mt-lineage A-1b (n = 9)				mt-lineage A-2Rt (n = 12)							
<i>16S</i>	-1.307	1612	285	115	0.998	0.024	44	15	0.980	0.006	50	9	1.000	0.010	51	20	0.970	0.010				
<i>ND1</i>	-0.816	967	287	104	0.997	0.047	44	14	0.974	0.010	70	9	1.000	0.026	53	10	0.970	0.016				
<i>NCX1 (SLC8A1)</i>	-0.648	505	26	37	0.851	0.006	7	5	0.651	0.003	3	4	0.525	0.002	5	4	0.649	0.003				
<i>NFIA</i>	-1.626	414	18	21	0.735	0.003	3	5	0.548	0.002	3	4	0.700	0.003	2	3	0.177	0.000				
<i>POMC</i>	-1.538	475	40	48	0.870	0.007	9	6	0.712	0.004	7	6	0.775	0.004	12	10	0.859	0.006				
<i>SLC8A3 (NCX3)</i>	-1.429	524	21	23	0.786	0.003	3	4	0.236	0.001	2	3	0.242	0.000	8	6	0.659	0.002				
<i>TYR</i>	-1.210	318	50	97	0.955	0.017	17	12	0.867	0.013	15	12	0.958	0.018	20	15	0.946	0.018				
	mt-lineage A-2Rs (n = 9)						mt-lineage A-3 (n = 12)				mt-lineage A-4 (n = 3)				mt-lineage A-5 (n = 5)							
<i>16S</i>	26	7	0.964	0.006	43	12	1.000	0.009	7	2	0.667	0.003	41	5	1.000	0.012						
<i>ND1</i>	38	7	0.964	0.016	37	8	0.939	0.013	9	2	0.667	0.006	38	4	0.900	0.018						
<i>NCX1 (SLC8A1)</i>	2	2	0.125	0.001	2	3	0.163	0.000	3	2	0.533	0.003	3	3	0.607	0.002						
<i>NFIA</i>	1	2	0.125	0.000	2	3	0.163	0.000	2	3	0.600	0.002	1	2	0.250	0.001						
<i>POMC</i>	6	5	0.556	0.003	9	5	0.652	0.004	3	2	0.533	0.003	4	3	0.607	0.003						
<i>SLC8A3 (NCX3)</i>	1	2	0.125	0.000	2	3	0.554	0.001	1	2	0.533	0.001	1	2	0.571	0.001						
<i>TYR</i>	11	4	0.442	0.008	9	5	0.493	0.007	1	2	0.533	0.002	12	7	0.964	0.018						
	mt-lineage A-6 (n = 8)						mt-lineage A-7 (n = 7)				mt-lineage A-8 (n = 3)				mt-lineage A-9a (n = 8)							
<i>16S</i>	25	8	1.000	0.005	27	7	1.000	0.006	3	2	0.667	0.001	28	7	0.964	0.006						
<i>ND1</i>	15	6	0.964	0.005	32	7	1.000	0.011	3	2	0.667	0.002	21	7	0.964	0.006						
<i>NCX1 (SLC8A1)</i>	4	5	0.505	0.002	2	3	0.538	0.001	4	3	0.733	0.004	6	6	0.792	0.004						
<i>NFIA</i>	2	3	0.425	0.001	2	3	0.275	0.001	2	3	0.600	0.002	2	3	0.433	0.001						
<i>POMC</i>	9	7	0.850	0.006	-	1	-	-	4	3	0.600	0.003	2	3	0.242	0.001						
<i>SLC8A3 (NCX3)</i>	2	2	0.363	0.001	2	2	0.440	0.002	-	1	-	-	1	2	0.264	0.001						
<i>TYR</i>	16	13	0.975	0.016	9	7	0.846	0.009	10	4	0.800	0.013	11	7	0.692	0.009						
	mt-lineage A-9b (n = 5)						mt-lineage A-9c (n = 6)				mt-lineage B-1 (n = 3)				mt-lineage B-2a (n = 12)							
<i>16S</i>	44	5	1.000	0.014	41	5	0.933	0.014	4	3	1.000	0.002	36	10	0.970	0.007						
<i>ND1</i>	36	5	1.000	0.018	39	4	0.800	0.023	-	1	-	-	42	10	0.970	0.013						
<i>NCX1 (SLC8A1)</i>	5	5	0.822	0.003	6	7	0.879	0.003	-	1	-	-	2	3	0.636	0.002						
<i>NFIA</i>	2	2	0.200	0.001	4	5	0.756	0.004	1	2	0.333	0.001	1	2	0.228	0.001						

<i>POMC</i>	6	3	0.378	0.003	7	5	0.742	0.006	8	5	0.933	0.008	9	7	0.851	0.004
<i>SLC8A3 (NCX3)</i>	3	4	0.644	0.001	-	1	-	-	3	4	0.867	0.003	4	5	0.361	0.002
<i>TYR</i>	12	9	0.978	0.013	11	6	0.848	0.014	6	5	0.933	0.009	10	9	0.812	0.010

	<u>mt-lineage B-2b (n = 8)</u>				<u>n-cluster I (n = 68)</u>				<u>n-cluster II (n = 56)</u>			
<i>16S</i>	24	7	0.964	0.006	204	61	0.996	0.026	176	53	0.997	0.018
<i>ND1</i>	33	7	0.964	0.014	218	57	0.994	0.049	192	47	0.994	0.037
<i>NCX1 (SLC8A1)</i>	7	6	0.833	0.005	19	26	0.875	0.005	12	13	0.483	0.002
<i>NFIA</i>	1	2	0.125	0.000	11	16	0.493	0.002	6	8	0.486	0.001
<i>POMC</i>	4	4	0.350	0.001	29	26	0.784	0.006	24	24	0.849	0.007
<i>SLC8A3 (NCX3)</i>	3	3	0.633	0.002	9	10	0.593	0.002	12	12	0.577	0.002
<i>TYR</i>	10	13	0.967	0.010	34	58	0.935	0.014	33	43	0.907	0.016

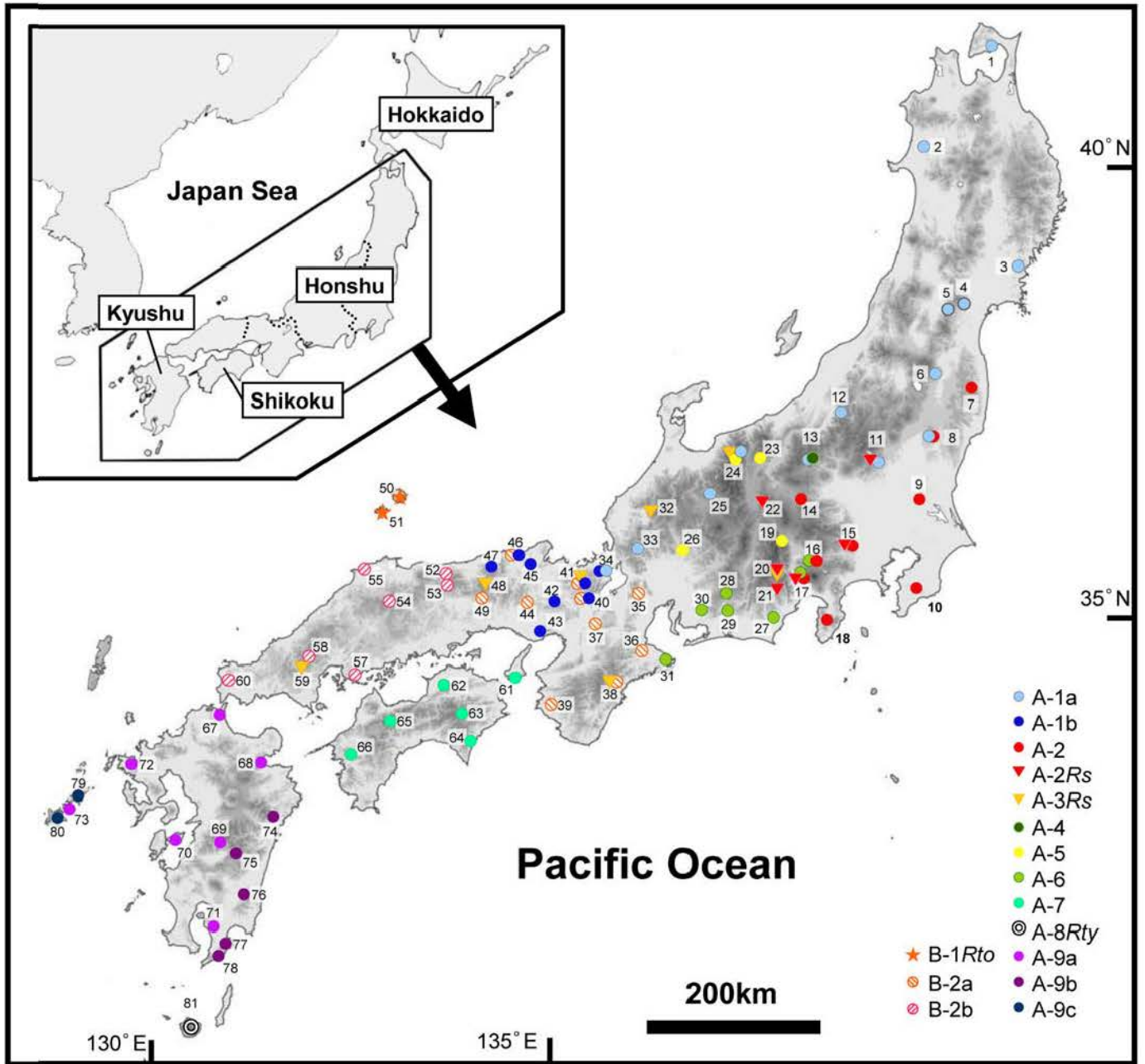


Fig. 1

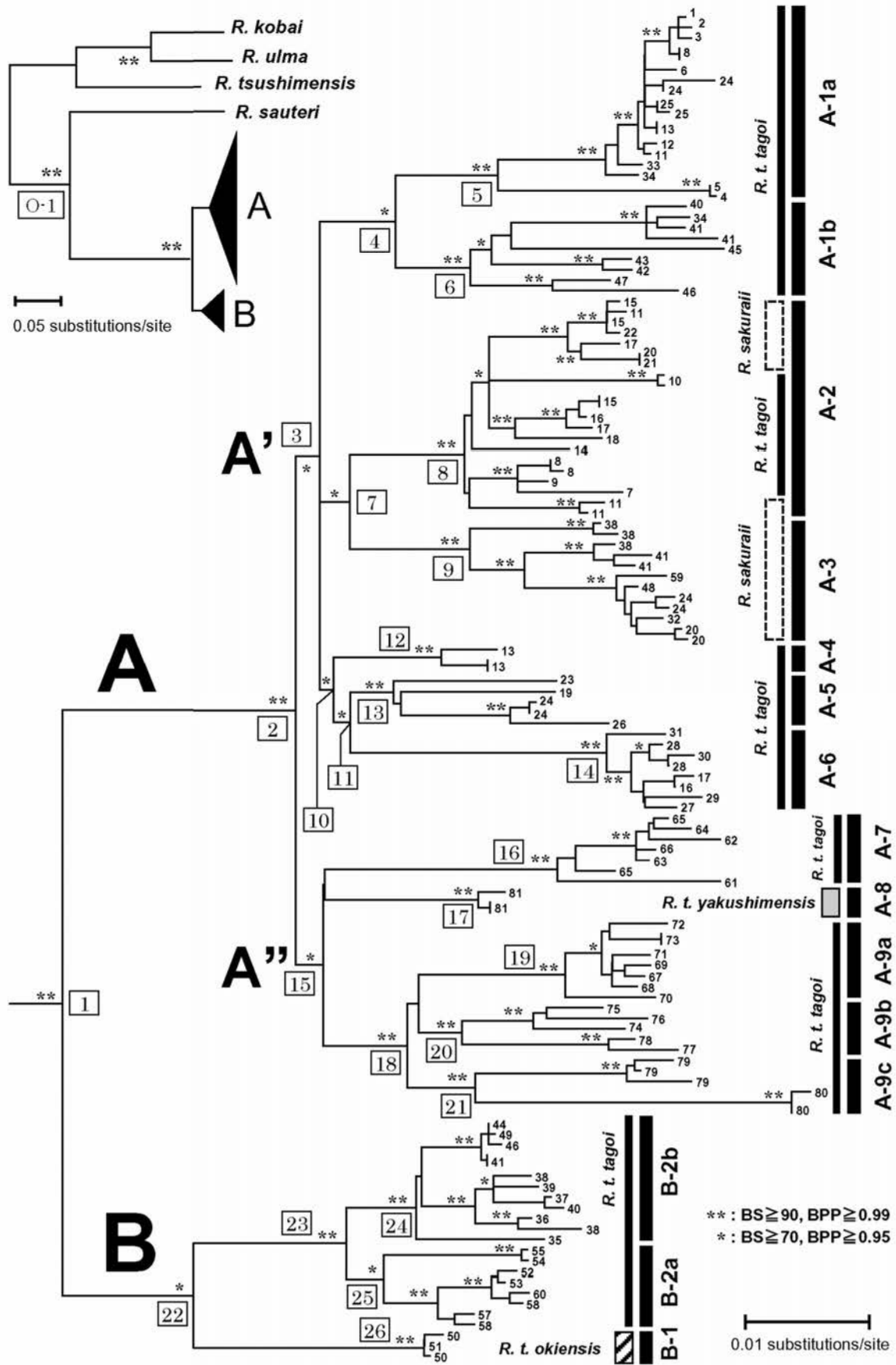


Fig. 2

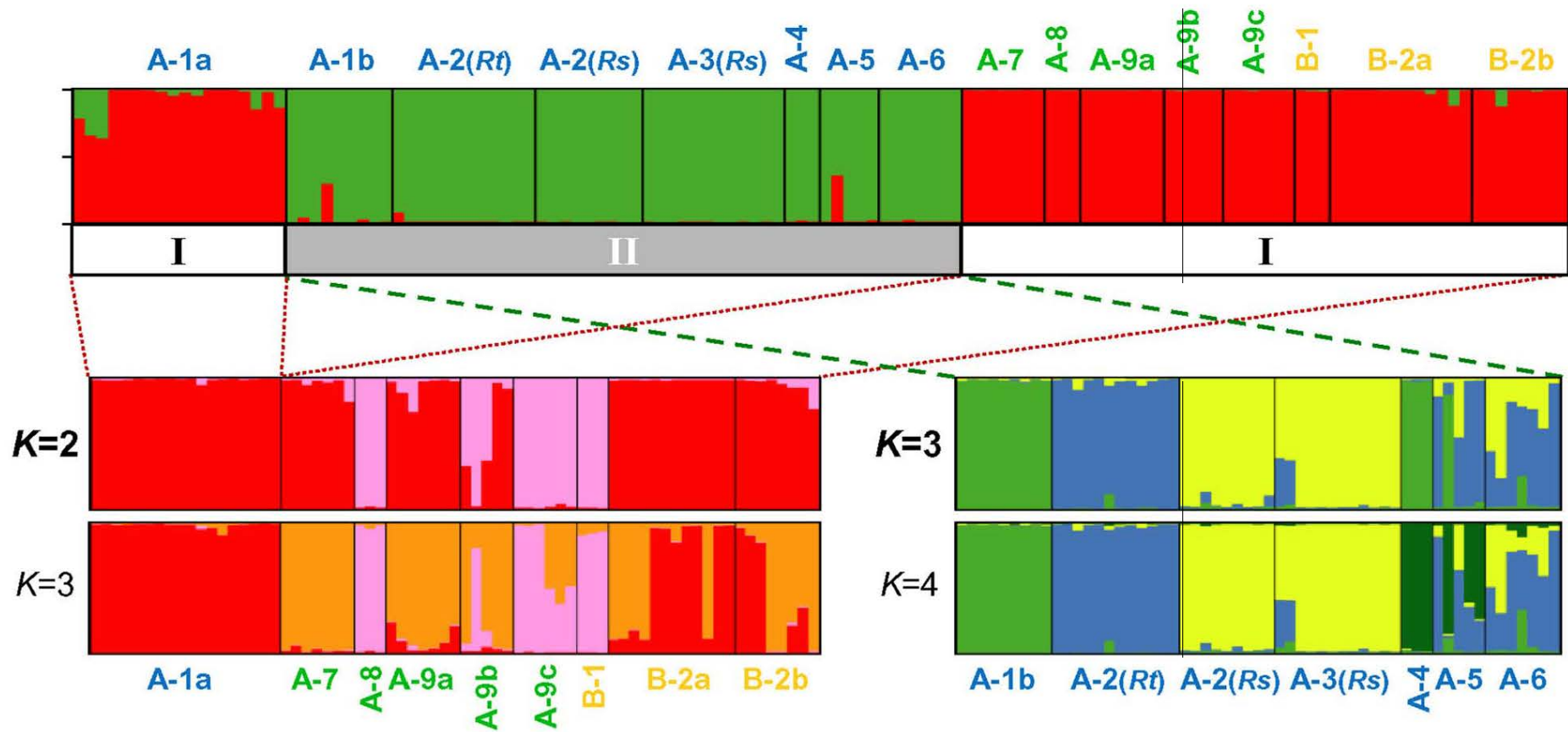
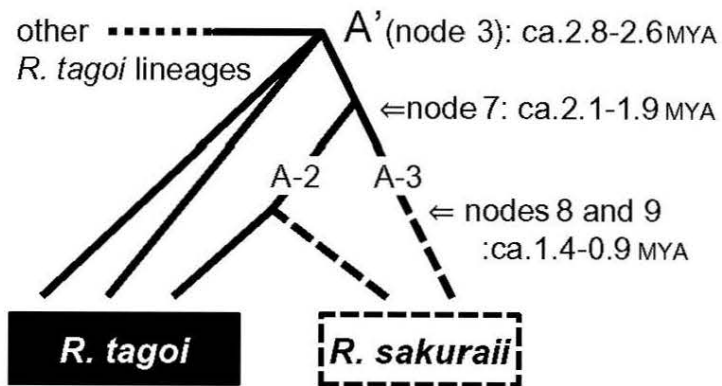


Fig. 3

1: ILS



2: introgression

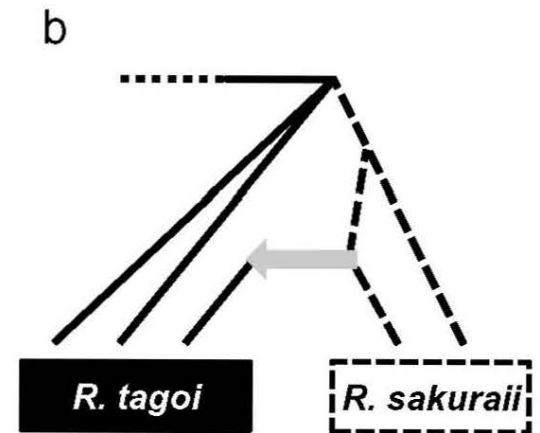
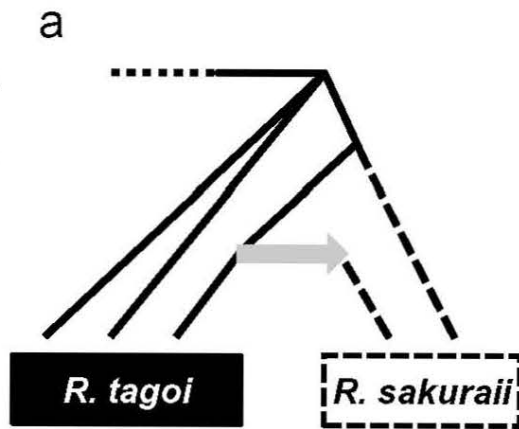


Fig. 4

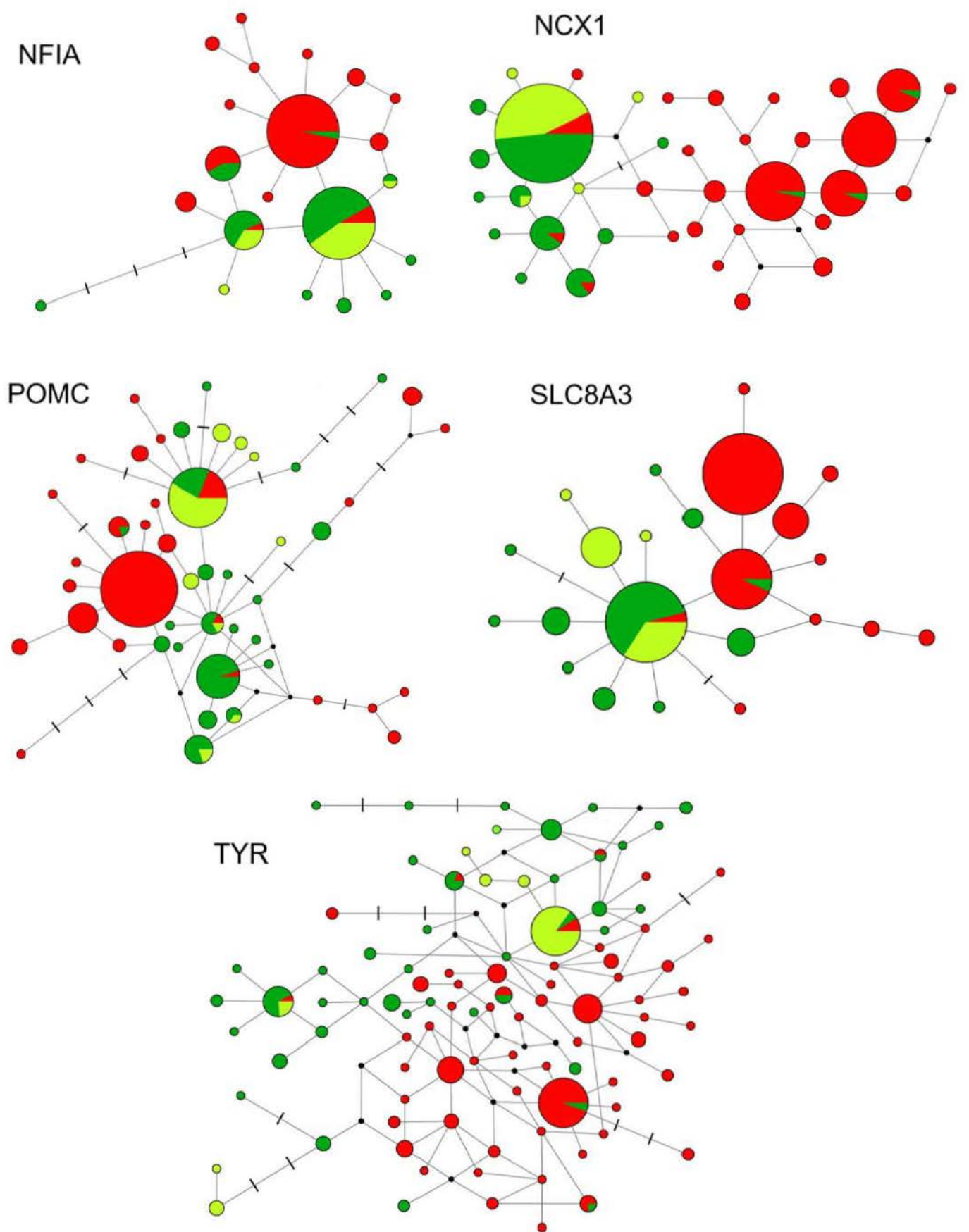


Fig. S1

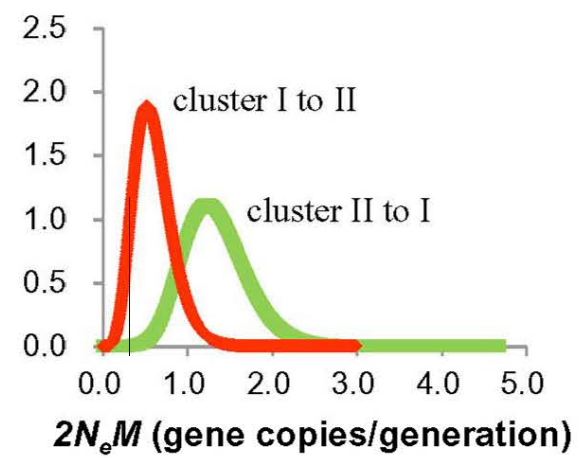
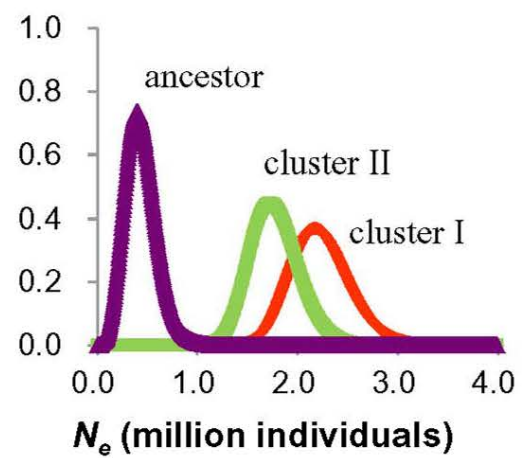
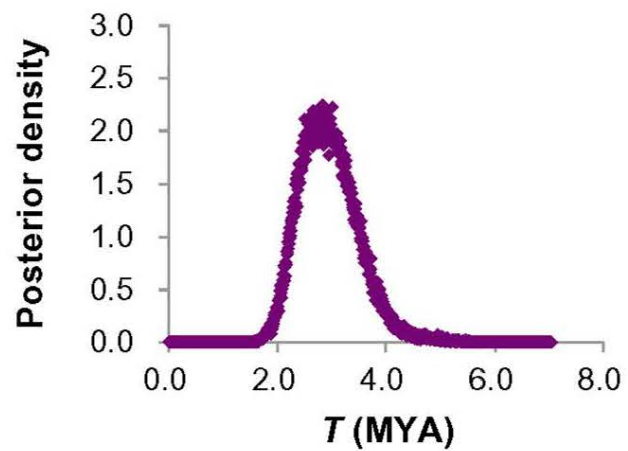


Fig. S2

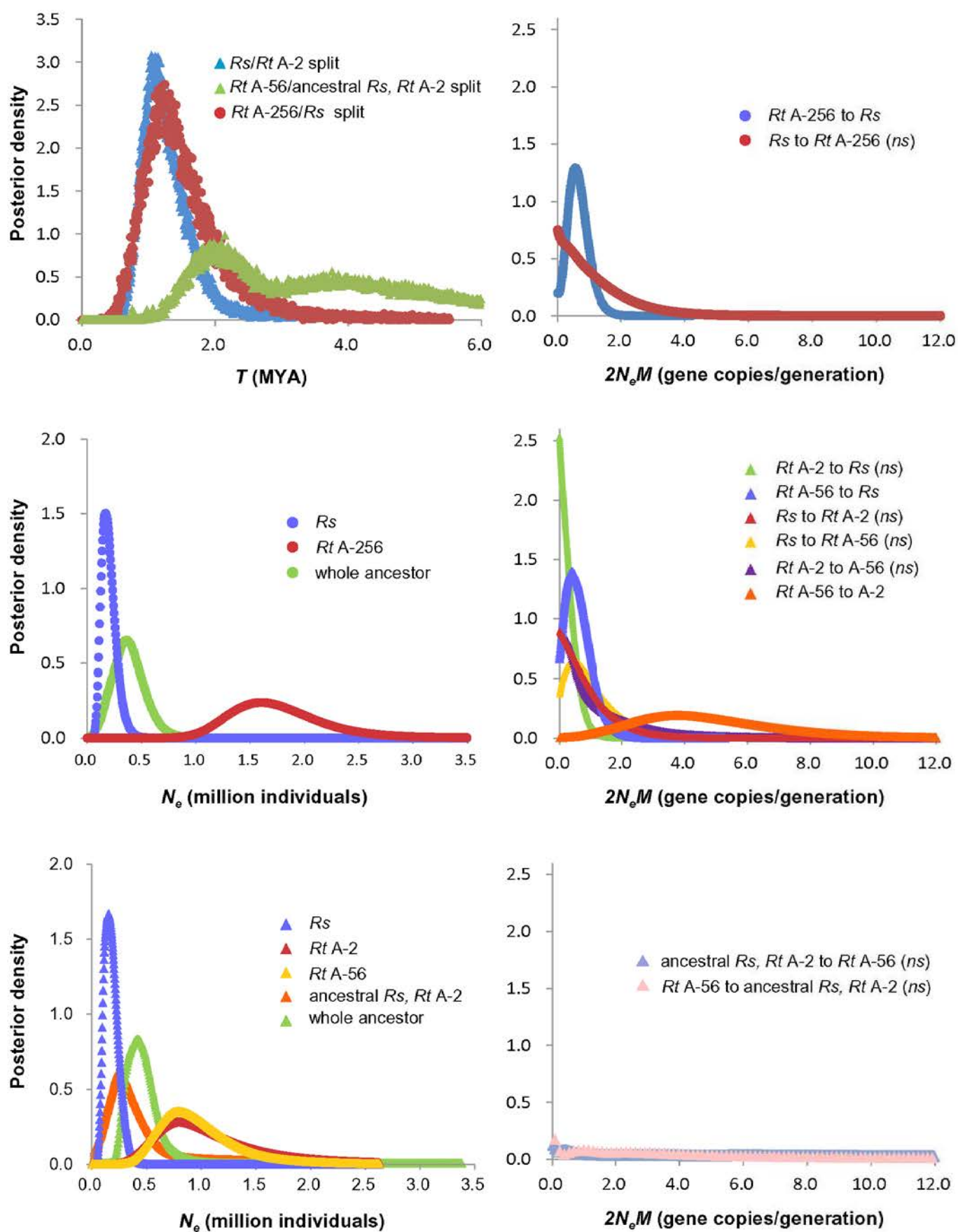
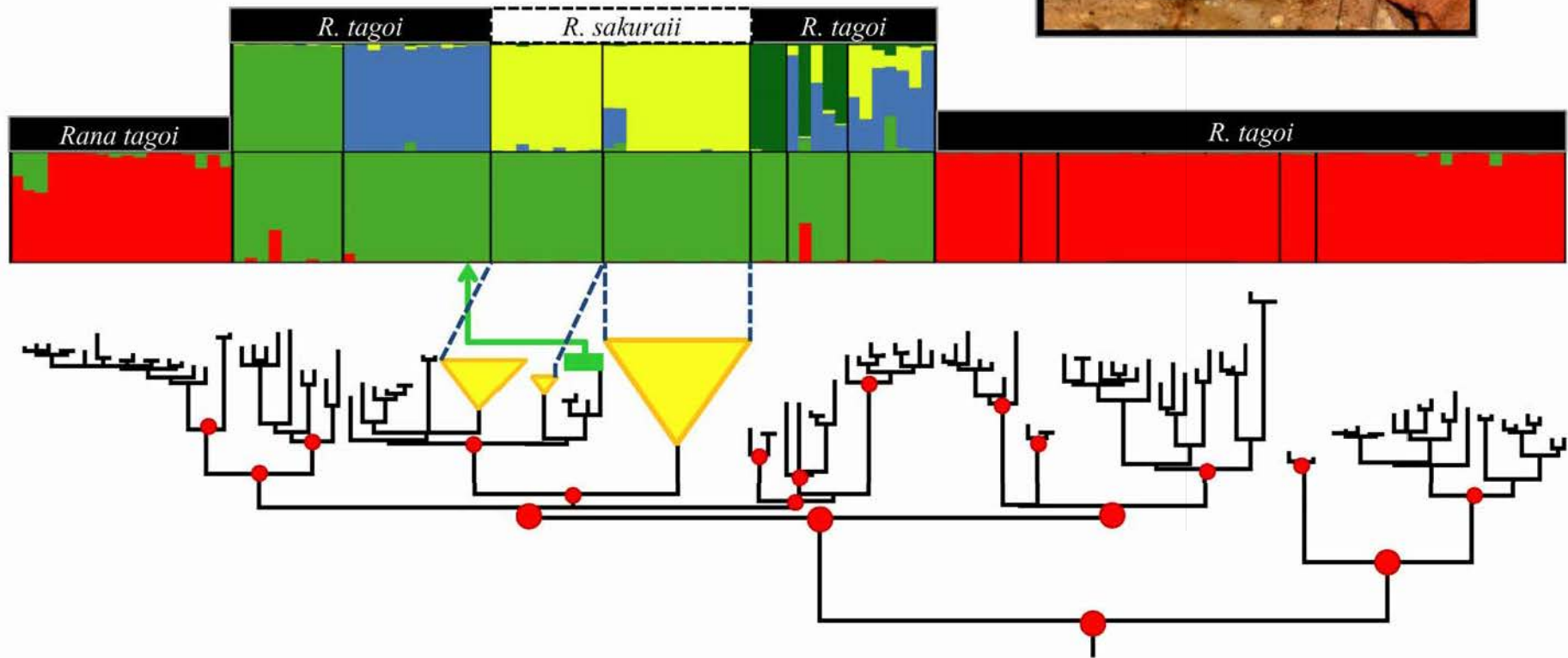


Fig. S3



Graphical abstract